Biotechnol Lett (2019) 41:1283–1298
https://doi.org/10.1007/s10529-019-02734-x

ORIGINAL RESEARCH PAPER

Design and in vitro delivery of HIV-1 multi-epitope DNA and peptide constructs using novel cell-penetrating peptides

Saba Davoodi · Azam Bolhassani · Seyed Mehdi Sadat · Shiva Irani

Received: 18 July 2019 / Accepted: 15 September 2019 / Published online: 17 September 2019

Abstract

Objectives Developing an effective HIV vaccine that stimulates the humoral and cellular immune responses is still challenging because of the diversity of HIV-1 virus, polymorphism of human HLA and lack of a suitable delivery system.

Results Using bioinformatics tools, we designed a DNA construct encoding multiple epitopes. These epitopes were highly conserved within prevalent HIV-1 subtypes and interacted with prevalent class I and II HLAs in Iran and the world. The designed DNA construct included $Nef_{60–84}$, $Nef_{126–144}$, $Vpr_{34–47}$, $Vpr_{60–75}$, $Gp160_{30–53}$, $Gp160_{308–323}$ and $P24_{8–151}$ epitopes (i.e., *nef-vpr-gp160-p24* DNA) which was cloned into pET-24a(+) and pEGFP-N1 vectors. The recombinant polyepitope peptide (rNef-Vpr-Gp160-P24; ~ 32 kDa) was successfully generated in *E. coli* expression system. The pEGFP-*nef-vpr-gp160-p24* and rNef-Vpr-Gp160-P24 polyepitope peptide were delivered into HEK-293 T cells using cell-penetrating peptides (CPPs). The MPG and HR9 CPPs, as well as the novel LDP-NLS and CyLoP-1 CPPs, were utilized for DNA and peptide delivery into the cells, respectively. SEM results confirmed the formation of stable MPG/pEGFP-N1-*nef-vpr-gp160-p24*, HR9/pEGFP-N1-*nef-vpr-gp160-p24*, LDP-NLS/rNef-Vpr-Gp160-P24 and CyLoP-1/rNef-Vpr-Gp160-P24 nanoparticles with a diameter of < 200 nm through non-covalent bonds. MTT assay results indicated that these nanoparticles did not have any major toxicity in vitro. Fluorescence microscopy, flow cytometry and western blot data demonstrated that these CPPs could significantly deliver the DNA and peptide constructs into HEK-293 T cells.

Conclusion The use of these CPPs can be considered as an approach in HIV vaccine development for in vitro and in vivo delivery of DNA and peptide constructs into mammalian cells.

Keywords HIV-1 · In silico studies · Cell penetrating peptides · Vaccine development

Electronic supplementary material The online version of this article (https://doi.org/10.1007/s10529-019-02734-x) contains supplementary material, which is available to authorized users.

S. Davoodi · S. Irani
Department of Biology, School of Basic Science, Science and Research Branch, Islamic Azad University, Tehran, Iran

A. Bolhassani (✉) · S. M. Sadat
Department of Hepatitis and AIDS, Pasteur Institute of Iran, Tehran, Iran
e-mail: azam.bolhassani@yahoo.com; A_bolhasani@pasteur.ac.ir

Introduction

Human immunodeficiency virus (HIV) is a cause of acquired immunodeficiency syndrome (AIDS) around the world. Generally, there are two types of HIV (e.g.,

HIV-1 and HIV-2). HIV-1 is more pathogenic and also the cause of most cases of AIDS in the world (Requejo 2006). HIV encodes three main genes (*gag*, *pol* and *env*) and five accessory genes (*vpr*, *vpu*, *vif*, *nef*, *rev* and *tat*), which play an important role in the replication and pathogenesis of the virus (Chiozzini and Toschi 2015). The *gag* gene encodes Gag precursor that is processed to the matrix proteins (p17), capsid (p24), nucleocapsid (p7) and p6 protein. The *pol* gene encodes Pol precursor, which is processed to protease, reverse transcriptase and integrase. The *env* gene encodes Env (gp160) glycoprotein that is processed to surface (gp120) and transmembrane (gp41) components (Miller and Sarver 1997). Nef is a cytoplasmic protein ($\sim$ 27–34 kDa) that is associated with the cell membrane (Kaminchik et al. 1994; Kelly et al. 2008). The progression of HIV infection in humans and animal models is closely related to the Nef protein (Hanna et al. 1998). Nef protein appears to activate the signaling pathways of T cells (Wei et al. 2003). The *vpr* gene encodes an accessory Vpr protein (viral protein R) that increases the replication and pathogenicity of the virus. The Vpr protein has a role in the viral complex entry into the nucleus and stops the cell cycle at the G2 stage. Vpr protein has inhibitory effects on the acquired immune system and causes T cells' apoptosis (Goede et al. 2015).

High genetic variability is one of the HIV-1 properties (Esteves et al. 2002). This high variability has caused some problems in the prevention, diagnosis, and treatment of AIDS and scientists are trying to develop an effective vaccine (Esparza 2013). An ideal HIV vaccine should stimulate humoral and cellular immune responses (Li et al. 2012). To solve the variability problem, various strategies have been used to develop T-cell-based vaccines (Perrin et al. 2010). One of these strategies is the design of a vaccine targeting the conserved epitopes inducing humoral and cellular immunity (Kunwar et al. 2013). Another important advance in development of an HIV vaccine is DNA vaccines encoding the immunogenic antigen (Arnon and Ben-Yedidia 2003). Most of these vaccines are safe in animal models (Chinombe and Ruhanya 2015) and they can be produced using various HIV proteins and the recombinant DNA technology (Puls and Emery 2006).

The low ability of drugs to penetrate into the cells led to a lack of biological function, reduced therapeutic efficacy, and increased toxicity. In recent years, various delivery techniques have been developed, but most of these techniques are toxic to cells and reduce cell viability (Zorko and Langel 2005). Recent studies have shown that some peptides have domains that can transfer protein through the cell membrane (Lundberg and Langel 2003). These peptides are known as cell-penetrating peptides (CPPs), which are < 30 amino acids long, and have high basic amino acids leading to their positive charge. The advantage of CPPs versus other delivery methods is high penetration into the cell, high cargo capacity, and low cytotoxicity (Temsamani and Vidal 2004). CPPs are capable of transporting a large number of cargoes, including small molecules, nucleic acids, proteins, viruses, imaging agents and drugs into the cells (Guidotti et al. 2017). CPPs were divided into three groups of protein-derived CPPs (e.g., Tat and Penetratin), chimeric CPPs (e.g., Transportan), and synthetic CPPs (e.g., oligoarginines) based on their origin (Milletti 2012). Based on physical and chemical properties, CPPs were classified into cationic (e.g., HR9 and CyLoP-1), amphipathic (e.g., MPG) and hydrophobic (e.g., Pep-1) groups (Pooga and Langel 2015). Nuclear localization sequences (NLS) are a group of short cationic CPPs that can enter the nucleus through nuclear pores and increase the penetration of CPPs into the cells (Ragin et al. 2002).

Bioinformatics methods are used for in silico analysis of biomolecules using statistical techniques (Khairkhah et al. 2018). CABS-dock is a server for modeling of protein-peptide interactions. This server is able to predict the 3D structure of the complexes that is close to their native structure (Kurcinski et al. 2015). Using bioinformatics tools and CABS-dock, we designed a polyepitope DNA construct containing the conserved immunogenic epitopes of HIV-1 subtypes which has interactions with prevalent HLAs in Iran and the world. Besides, we used MPG and HR9 CPPs for DNA delivery, and CyLoP-1 and LDP-NLS CPPs for peptide delivery into HEK-293 T cells for development of HIV-1 therapeutic vaccine in near future.

Materials and methods

Design of polyepitope DNA constructs

To design polyepitope DNA construct, the reference sequences of HIV-1 Nef, Vpr, Gp160, and P24

proteins were obtained from the UniProt database (www.uniprot.org). The protein sequences were compared with the sequences recorded in the HIV Molecular Immunology Database (www.hiv.lanl.gov). All immunization sequences recorded in the database were extracted from the Immune Epitope Database (IEDB) (www.iedb.org). The peptide sequences were checked if they bind to class I and II MHC molecules by NET MHC database (https://www.cbs.dtu.dk/services/NetMHC/), and the selected epitopes were categorized. Processing (TAP transport and Proteasomal cleavage) of the selected epitopes were predicted using the IEDB database. The selected epitopes were compared with the previously reported sequences that had better scores and finally, dominant epitopes were selected for each protein. Then, the selected epitopes were checked if they bind to B cells (https://www.cbs.dtu.dk/services/BepiPred/). Epitope Conservancy Analysis among HIV subtypes and population coverage was performed using the IEDB website (Khairkhah et al. 2018). Interaction between the selected epitopes and MHCs was studied by the CABS-dock peptide-protein docking website. Finally, the peptide construct (Nef-Vpr-Gp160-P24) was designed using the selected epitopes. The DNA construct (*nef-vpr-gp160-p24*) was ordered and synthesized in the pUC57 cloning vector by Biomatik Corporation (Canada).

Peptides and plasmids

Primary amphipathic MPG (GALFLGFLGAAGST MGAWSQPKKKRKV), HR9 (CHHHHRRRRRRR RRHHHHHC), Cysteine-rich CyLoP-1 (CRWRWK CCKK) and LDP-NLS (KWRRKLKKLRPKKKR KV) peptides were synthesized by Biomatik Corporation (Canada, Table 1). Moreover, the pUC57 vector harboring the DNA construct (*nef-vpr-gp160-p24*) was synthesized by Biomatik Corporation (Canada). The pEGFP-N1 eukaryotic expression vector (Clontech, USA) and pET-24a(+) prokaryotic expression vector (Novagen, USA) were previously provided by our group.

Cloning of the DNA construct in pET-24a(+)

The DNA construct (*nef-vpr-gp160-p24*) was digested from the pUC57 cloning vector using *Bam*HI and *Hind*III restriction enzymes (Thermo Fisher Scientific) and subcloned into the *Bam*HI and *Hind*III cloning sites of pET-24a(+) prokaryotic expression vector using T4 DNA ligase (Thermo Fisher Scientific). The pET-24a(+) vector is 5310 bp containing a kanamycin resistance gene and a histidine-tag which its promoter is regulated by Isopropyl β-D-1-thiogalactopyranoside (IPTG; www.snapgene.com). The pET-24a(+) vector harboring the *nef-vpr-gp160-p24* gene construct was transferred into the competent DH5α *E. coli* using heat shock, and kanamycin resistant colonies were selected. The pET-24a(+)-*nef-vpr-gp160-p24* was extracted using the Plasmid DNA Extraction Mini Kit (FAVORGEN, Taiwan), and analyzed by agarose gel electrophoresis. The concentration and purity of the pET-24a(+)-*nef-vpr-gp160-p24* were determined using a NanoDrop spectrophotometer (Thermo Fisher Scientific). The presence of the *nef-vpr-gp160-p24* gene was confirmed by digestion with the restriction enzymes.

Cloning of the DNA construct in pEGFP-N1

The DNA construct (*nef-vpr-gp160-p24*) was digested from the pUC57 cloning vector using *Xho*I and *Hind*III restriction enzymes (Thermo Fisher Scientific) and subcloned into the *Xho*I and *Hind*III cloning sites of the pEGFP-N1 eukaryotic expression vector using T4 DNA ligase (Thermo Fisher Scientific). The pEGFP-N1 vector is 4733 bp containing a kanamycin resistance gene and an EGFP tag (www.snapgene.com). All processes of subcloning were similarly performed as mentioned in before section.

Expression of the polyepitope peptide in prokaryotic expression system

To produce the recombinant polyepitope peptide (rNef-Vpr-Gp160-P24), the *E. coli* Rosetta and BL21 strains were transformed with pET-24a(+) harboring the *nef-vpr-gp160-p24* gene construct. The recombinant clones were selected on LB (Luria–Bertani) agar (Sigma-Aldrich, Germany) plate containing kanamycin and transferred to Ty2x medium to an OD (optical density) of 0.7–0.8 at 600 nm. Then, 1 mM Isopropyl β-D-1-thiogalactopyranoside (IPTG, Sinaclon, Iran) was used at 37 °C to induce the expression of the polyepitope peptide. The cell pellet was analyzed by SDS-PAGE in a gel containing

Table 1 List of the peptides used in this study

Peptide	Sequence	Cargo	References
MPG	GALFLGFLGAAGSTMGAWSQPKKKRKV	DNA	(Morris 1997)
HR9	CHHHHHRRRRRRRRRHHHHHC	DNA	(Liu et al. 2015)
CyLoP-1	CRWRWKCCKK	Peptide	(Jha et al. 2011)
LDP-NLS	KWRRKLKKLRPKKKRKV	Peptide	(Ponnappan and Chugh 2017)

12.5% acrylamide, and western blot using an anti-His tag antibody (Abcam, USA).

Purification of the histidine-tagged polyepitope peptide

The rNef-Vpr-Gp160-P24 peptide was purified by an affinity chromatography technique using Ni–NTA agarose column (Macherey–Nagel) under denaturing conditions (i.e., 8 M urea buffer and pH 4.5) and Tris–HCl lysis buffer. Then, the recombinant peptide was dialyzed in phosphate buffered saline (PBS) solution using a 10 kDa dialysis membrane (Thermo Scientific). Finally, its concentration and purity were measured using the Bradford protein assay kit (Sigma, Germany) and NanoDrop spectrophotometer (Thermo Fisher Scientific). According to LAL assay, contamination with LPS was < 0.5 EU/mg (QCL-1000, Lonza).

Preparation of the MPG/DNA and HR9/DNA complexes and gel retardation assay

To form the MPG/pEGFP-N1-*nef-vpr-gp160-p24* and HR9/pEGFP-N1-*nef-vpr-gp160-p24* complexes, the MPG and HR9 peptides were mixed with an equal amount (2 μg) of pEGFP-N1-*nef-vpr-gp160-p24* at different nitrogen to phosphate ratios (N/P: 0.5, 1, 2, 5 and 10) and incubated at room temperature for 45 min. The formation of the complexes was investigated using gel retardation assay. For this purpose, 1% agarose gel was used to evaluate the electrophoretic mobility of the complexes.

Stability and protection assay of the MPG/DNA and HR9/DNA nanoparticles

To verify the stability of MPG/pEGFP-N1-*nef-vpr-gp160-p24* and HR9/pEGFP-N1-*nef-vpr-gp160-p24* complexes against DNA nucleases, DNase I was added to complexes with different N/P ratios (0.5, 1, 2, 5 and 10). The mixtures were incubated at 37 °C for 1 h and finally, the stop solution (200 mM sodium chloride, 20 mM EDTA and 1% SDS) was added to the mixtures. To evaluate the serum stability, MPG/pEGFP-N1-*nef-vpr-gp160-p24* and HR9/pEGFP-N1-*nef-vpr-gp160-p24* complexes with N/P ratios of 5 and 10, respectively were exposed to 10% serum at 37 °C for 5 h. Finally, pEGFP-N1-*nef-vpr-gp160-p24* was dissociated from the MPG and HR9 peptides using 10% SDS, and analyzed by 1% agarose gel electrophoresis (Motevalli et al. 2018).

Preparation of the CyLoP-1/peptide and LDP-NLS/peptide complexes

To form the CyLoP-1/rNef-Vpr-Gp160-P24 and LDP-NLS/rNef-Vpr-Gp160-P24 complexes, the CyLoP-1 and LDP-NLS CPPs were mixed with an equal amount (1 μg) of the rNef-Vpr-Gp160-P24 peptide at different CyLoP-1:rNef-Vpr-Gp160-P24 and LDP-NLS:rNef-Vpr-Gp160-P24 molar ratios (2:1, 5:1, 10:1, 15:1, 20:1, 30:1) and incubated for 60 min at room temperature. The formation of the complexes was confirmed by native PAGE and SDS-PAGE in a gel containing 12.5% acrylamide.

Physicochemical characterization of the complexes

The MPG/pEGFP-N1-*nef-vpr-gp160-p24*, HR9/pEGFP-N1-*nef-vpr-gp160-p24*, CyLoP-1/rNef-Vpr-Gp160-P24, and LDP-NLS/rNef-Vpr-Gp160-P24 nanoparticles were formed at the ratios of 10, 5, 10 and 10, respectively and their size and morphology were determined using scanning electron microscope (FEI Quanta 200 SEM, PHILIPS, USA). Moreover, the

charge of nanoparticles was assessed by Zetasizer Nano ZS (Malvern Instruments, UK) at 25 °C.

Cell culture

Human embryonic kidney cells (HEK-293 T, CRL-1651, Pasteur Institute of Iran) were cultured in RPMI-1640 medium (Sigma, Germany) supplemented with 5% FBS (Fetal Bovine Serum, Gibco, Germany) and 1% Gentamicin solution at 37 °C and 5% CO_2 and subcultured every 2 days. To perform MTT and transfection assay, the cells were seeded in 96-well (1×10^4 cells/well) and 24-well (5×10^4 cells/well) plates, respectively.

MTT assay

MTT assay was performed to evaluate the viability of the cells treated with the complexes. HEK-293 T cells (1×10^4 cells/well) were seeded in a 96-well plate (Greiner, Germany) and cultured for 24 h. The medium was replaced by fresh RPMI-1640. The MPG (41.5 μg), HR9 (9.3 μg), pEGFP-N1-*nef-vpr-gp160-p24* (2 μg), MPG/pEGFP-N1-*nef-vpr-gp160-p24* (N/P ratio of 10), HR9/pEGFP-N1-*nef-vpr-gp160-p24* (N/P ratio of 5), CyLoP-1 (10 μg), LDP-NLS (10 μg), rNef-Vpr-Gp160-P24 (1 μg), CyLoP-1/rNef-Vpr-Gp160-P24 (molar ratio of 10:1) and LDP-NLS/rNef-Vpr-Gp160-P24 (molar ratio of 10:1) were added to the cells and cultured for 48 h. Then, the medium was removed and MTT solution (5 mg/mL, Sigma) in RPMI-1640 was added to each well, and incubated for 3 h at 37 °C. After 3 h, the medium was removed and dimethyl sulfoxide (DMSO) (Sigma, Germany) was added to each well (100 μl) to dissolve the formazan crystals. The absorbance was measured by ELISA reader at 570 nm. Untreated cells and cells treated with 70% ethanol were considered as negative (100% cell viability) and positive controls, respectively. MTT assay was performed in triplicate.

Transfection of HEK-293Tcells with the MPG/DNA and HR9/DNA complexes

HEK-293 T cells (5×10^4 cells/well) were seeded in a 24-well microtiter plate (Greiner, Germany) and cultured for 24 h. The MPG/pEGFP-N1 and MPG/pEGFP-N1-*nef-vpr-gp160-p24* complexes were prepared at the N/P ratio of 10. Then, the medium was removed and the complexes were added to cells in a serum-free medium, and the cells were incubated at 37 °C for 6 h. After 6 h, the medium was replaced with complete RPMI-1640 medium supplemented with 5% FBS and the cells were incubated at 37 °C for 48 h. The HR9/pEGFP-N1 and HR9/pEGFP-N1-*nef-vpr-gp160-p24* complexes were prepared at the N/P ratio of 5. Then, the medium was removed and the complexes were added to cells in a serum-free medium, and the cells were incubated at 37 °C for 1 h. After 1 h, the complete RPMI-1640 medium supplemented with 10% FBS was added to the cells, and the cells were incubated at 37 °C for 48 h. The cells treated with TurboFect (Fermentas)/pEGFP-N1 and TurboFect/pEGFP-N1-*nef-vpr-gp160-p24* complexes were considered as positive controls, and the untreated cells were considered as a negative control. The transfection efficiency of cells treated with the complexes was evaluated by Fluorescence microscope (Envert Fluorescent Ceti, Korea) and FACS Calibur flow cytometer (Partec, Germany). Expression of the Nef-Vpr-Gp160-P24 construct was evaluated by western blot using an anti-His-tag antibody (Abcam, USA).

Transfection of HEK-293 T cells with the CyLoP-1/peptide and LDP-NLS/peptide complexes

HEK-293 T cells (5×10^4 cells/well) were seeded in a 24-well microtiter plate (Greiner, Germany) and cultured for 24 h. The CyLoP-1/rNef-Vpr-Gp160-P24 and LDP-NLS/rNef-Vpr-Gp160-P24 complexes were prepared at a molar ratio of 10:1. Then, the medium was removed and the complexes were added to cells in a serum-free medium, and the cells were incubated at 37 °C for 2 h. After 2 h, the cells were treated with trypsin–EDTA and harvested by centrifugation. The cells treated with TurboFect (ProJect, Fermentas)/rNef-Vpr-Gp160-P24 complexes were considered as a positive control, and the untreated cells were considered as a negative control. Transfection efficiency of the cells treated with the complexes was evaluated by western blot using an anti-His-tag antibody (Abcam, USA).

Statistical analysis

Prism 5.0 software (GraphPad, San Diego, California, USA) was used for statistical analysis (Student's t-test). The value of $p < 0.05$ was considered

statistically significant. Each experiment was repeated two times.

Results

Design of the peptide construct

The Nef, Vpr, Gp160 and P24 epitopes which had the highest MHCI and MHCII binding level were selected from the NET MHC database. The results of population coverage showed that the selected epitopes could specifically bind to common HLA molecules in target populations. The top immunodominant epitopes were selected for the design of the polyepitope peptide construct (Table 2). Interaction between the selected epitopes and common HLAs were checked by CABS-dock peptide-protein docking website and top models for the interaction of each peptide and HLA. Top-ranked models in CABS-dock have higher Cluster Density (CD). CD is the number of elements in a cluster divided by its average root-mean-square deviation (N/average RMSD). RMSD was used to measure docking quality. Based on RMSD, the accuracy of docking is divided into three categories of high accuracy (RMSD < 3 Å), moderate accuracy (3 Å $\leq$ RMSD $\leq$ 5.5 Å and low accuracy (RMSD > 5.5 Å) (Kurcinski et al. 2015). CD and average RMSD of epitope-HLAI and epitope-HLAII dockings were shown in Tables 3 and 4, respectively. Further information was provided in Supplementary Tables (Tables S1 and S2). Figure 1 is an example of two peptide-protein dockings between $Vpr_{60–75}$-HLA-A*0201 and Vpr_{60-75}-HLA-DRB1*0301. Finally, the polyepitope peptide construct was designed using the selected $Nef_{60–84}$, $Nef_{126–144}$, $Vpr_{34–47}$, $Vpr_{60–75}$, $Gp160_{30–53}$, $Gp160_{308–323}$ and $P24_{8–151}$ epitopes (Fig. 2). The $P24_{8–151}$ was highly immunogenic and used as a long peptide.

Table 2 The selected epitopes for the design of the polyepitope peptide construct

Protein	Position	Epitope sequence
Nef	60–84	QEEEEVGFPVTPQVPLRPMTYKAAV
Nef	126–144	YTPGPGVRYPLTFGWCYKL
Vpr	34–47	FPRIWLHGLGQHIY
Vpr	60–75	IIRILQQLLFIHFRIG
Gp160	30–53	ATEKLWVTVYYGVPVWKEATTLFC
Gp160	308–323	RIQRGPGRAFVTIGKI
P24	8–151	(www.uniprot.org)

Cloning of the DNA construct in pET-24a(+) and pEGFP-N1

The DNA construct encoding *nef-vpr-gp160-p24* gene was cloned into pET-24a(+) and pEGFP-N1 vectors. The presence of the *nef-vpr-gp160-p24* gene construct in pET-24a(+) and pEGFP-N1 was confirmed by digestion with *Bam*HI and *Hind*III, and *Xho*I and *Hind*III, respectively, and also sequencing. The *nef-vpr-gp160-p24* gene was observed as a clear band of $\sim$ 867 bp in 1% agarose gel (Fig. 3).

Expression and purification of the polyepitope peptide

The optimum expression of the rNef-Vpr-Gp160-P24 peptide was observed in Rosetta strain at 37 °C and 4 h after induction (Fig. 4a). The rNef-Vpr-Gp160-P24 peptide was purified under denaturing conditions. The rNef-Vpr-Gp160-P24 peptide was observed as a clear band of $\sim$ 32 kDa in SDS-PAGE (Fig. 4b). The purified peptide was detected and confirmed by western blot analysis (Fig. 4c). The concentration of the peptide was between 0.5 and 0.7 mg/mL.

Gel retardation, stability and protection assay of the MPG/DNA and HR9/DNA nanoparticles

Gel retardation assay showed that DNA did not migrate in agarose gel at N/P ratio of 10 (in complex with MPG), and 5 (in complex with HR9) indicating the formation of MPG/pEGFP-N1-*nef-vpr-gp160-p24* and HR9/pEGFP-N1-*nef-vpr-gp160-p24* complexes, respectively (Fig. 5). After treatment with DNase I, pEGFP-N1-*nef-vpr-gp160-p24* (control) was degraded rapidly, while the DNA in MPG/pEGFP-N1-*nef-vpr-gp160-p24* (N/P ratio of 10) and HR9/pEGFP-N1-*nef-vpr-gp160-p24* (N/P ratio of 5) complexes remained intact. The serum protection assay also showed that pEGFP-N1-*nef-vpr-gp160-p24* (control) was degraded after 5 h of incubation with FBS, but the DNA in MPG/pEGFP-N1-*nef-vpr-gp160-P24* (N/P ratio of 10) and HR9/pEGFP-N1-*nef-vpr-gp160-p24* (N/P ratio of 5) complexes remained intact (data not shown).

Table 3 Cluster density and average RMSD of top-ranked CABS-dock models of peptide-HLA I complexes

Epitope	HLA-A*0101	HLA-A*0201	HLA-A*0301	HLA-A*1101	HLA-A*2402	HLA-B*0702	HLA-B*0801	HLA-B*2705	HLA-B*3501	HLA-B*5101	Average
Cluster density											
Nef60–84	51.4	53.5	52.38	80.35	49.62	58.95	41.42	49.74	70.47	50.87	55.87
Nef126–144	52.74	51.67	24.63	48.67	32.78	48.43	40.73	28.7	50.48	58.91	43.77
Vpr34–47	51.33	82.5	49.85	50.49	48.2	37.56	62.22	46.99	52.45	61.62	54.32
Vpr60–75	88.59	59.42	44.73	33.36	59.84	57.75	64.09	97.96	51.89	42.59	60.02
Gp16030–53	38.56	78.72	77.45	72.27	35.17	46.44	35.04	68.98	75.72	43.13	57.15
Gp160308–323	76.51	48.25	29.92	63.52	45.73	48.25	35.99	48.67	44.51	79.5	52.08
Average RMSD											
Nef60–84	1.21	1.98	1.99	0.71	2.06	2.19	2.75	2.29	1.42	2.02	1.86
Nef126–144	1.92	1.99	4.83	2.01	3.14	2.17	2.38	3.34	4.6	2.27	2.87
Vpr34–47	1.97	1.22	2.59	4	2.3	2.9	2.12	1	2.23	0.8	2.11
Vpr60–75	1.13	0.86	2.48	4.38	1.77	3.31	1.75	1.33	2.39	4.37	2.38
Gp16030–53	3.11	1.3	1.3	0.72	2.84	2.17	3	1.46	1.41	3.34	2.07
Gp160308–323	1.52	3.81	2.91	2.06	2.21	1.18	2.97	3.95	2.45	1.31	2.44

Table 4 Cluster density and average RMSD of top-ranked CABS-dock models of peptide-HLA II complexes

Epitope	HLA-DRB1*0101	HLA-DRB1*0301	HLA-DRB1*0401	HLA-DRB1*1501	HLA-DRB5*0101	Average
Cluster density						
Nef60–84	23.53	27.9	38.73	28.06	32.53	30.15
Nef126–144	60.03	111	123.54	73.5	62.25	86.07
Vpr34–47	58.38	51.59	70.89	238.72	59.62	95.84
Vpr60–75	162.51	61.67	57.54	113.72	43.87	87.86
Gp16030–53	49.56	56.27	31.44	38.67	37.03	42.59
Gp160308–323	59.21	35.44	44.25	36.66	36.56	42.42
Average RMSD						
Nef60–84	2.72	3.69	0.83	3.49	2.83	2.71
Nef126–144	1.68	0.9	0.81	1.97	3.95	1.86
Vpr34–47	1.8	2.42	1.1	0.42	3.37	1.82
Vpr60–75	0.47	1.9	2.24	0.75	3.01	1.67
Gp16030–53	2.02	1.08	5.25	2.61	3.02	2.8
Gp160308–323	1.72	5.62	3.05	3.68	2.74	3.36

Formation of the CyLoP-1/peptide and LDP-NLS/peptide complexes

The CyLoP-1/rNef-Vpr-Gp160-P24 complexes were observed as two separate bands of ~ 32 kDa (rNef-Vpr-Gp160-P24) and ~ 1.4 kDa (CyLoP-1) in SDS-PAGE (Fig. 6a). The LDP-NLS/rNef-Vpr-Gp160-P24 complexes were observed as two separate bands of ~ 32 kDa (rNef-Vpr-Gp160-P24) and ~ 2.3 kDa (LDP-NLS) in SDS-PAGE gel (Fig. 6b). These results indicated non-covalent interactions between polyepitope peptide and CPPs at molar ratios of 1:2, 1:5, 1:10, 1:15, 1:20 and 1:30 (peptide: CPP). The CyLoP-1/rNef-Vpr-Gp160-P24 (Fig. 6c) and LDP-NLS/rNef-Vpr-Gp160-P24 (Fig. 6d) complexes were observed as single band in native PAGE gel indicating the complex formation.

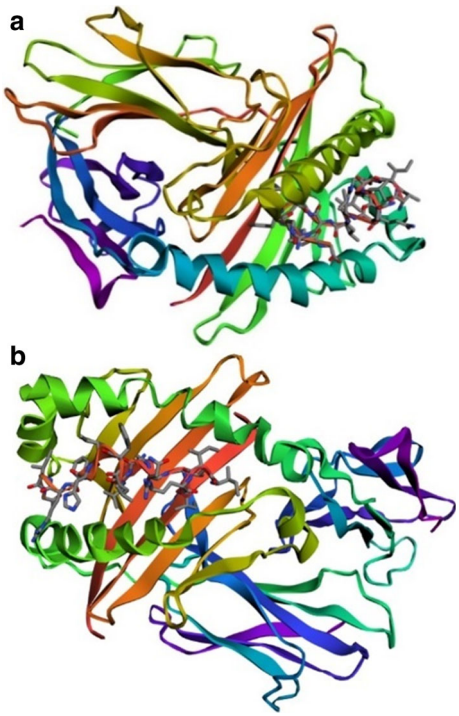

Fig. 1 Two peptide-protein docking models: **a** the top-ranked CABS-dock model of $Vpr_{60–75}$-HLA-A*0201 complex with 51 elements, average RMSD of 0.86 and cluster density of 59.42; **b** the top-ranked CABS-dock model of $Vpr_{60–75}$-HLA-DRB1*0301 complex with 117 elements, average RMSD of 1.90 and cluster density of 61.67

Physicochemical characterization of the complexes

The size and morphology of nanoparticles were investigated by SEM. The pEGFP-N1-*nef-vpr-gp160-p24* (Fig. 7a) and MPG (Fig. 7b) formed spherical MPG/pEGFP-N1-*nef-vpr-gp160-p24*

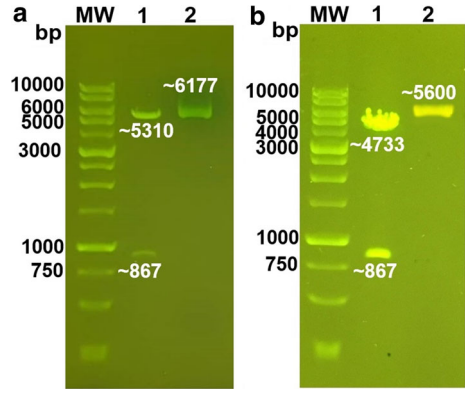

Fig. 3 Cloning of the DNA construct in **a** pET-24a(+) and **b** pEGFP-N1: **a** Lane 1: double digested pET-24a(+) (∼ 5310 bp) and *nef-vpr-gp160-p24* gene (∼ 867 bp) using *Bam*HI and *Hind*III restriction enzymes, Lane 2: The purified pET-24a(+)-*nef-vpr-gp160-p24* (∼ 6177 bp); **b** Lane 1: Double digested pEGFP-N1 (∼ 4733 bp) and *nef-vpr-gp160-p24* gene (∼ 8 67 bp) using *Xho*I and *Hind*III restriction enzymes, Lane 2: The purified pEGFP-N1-*nef-vpr-gp160-p24* (∼ 5600 bp); MW: Molecular weight marker (DNA ladder, 1 kb, SMOBIO)

complexes (N/P: 10) with an average diameter of ∼ 150–200 nm (Fig. 7d). HR9 (Fig. 7c) and pEGFP-N1-*nef-vpr-gp160-p24* (Fig. 7a) formed nonspherical HR9/pEGFP-N1-*nef-vpr-gp160-p24* complexes (N/P: 5) with an average diameter of ∼ 150–200 nm (Fig. 7e). CyLoP-1 (Fig. 8b) and rNef-Vpr-Gp160-P24 (Fig. 8a) formed spherical CyLoP-1/rNef-Vpr-Gp160-P24 complexes (molar ratio of 10) with an average diameter of ∼ 100–200 nm (Fig. 8d). LDP-NLS (Fig. 8c) and rNef-Vpr-Gp160-P24 (Fig. 8a) formed nonspherical LDP-NLS/rNef-Vpr-Gp160-P24 complexes (molar ratio of 10) with an average diameter of ∼ 100–150 nm (Fig. 8e). Besides, the zeta potential of the complexes was studied by

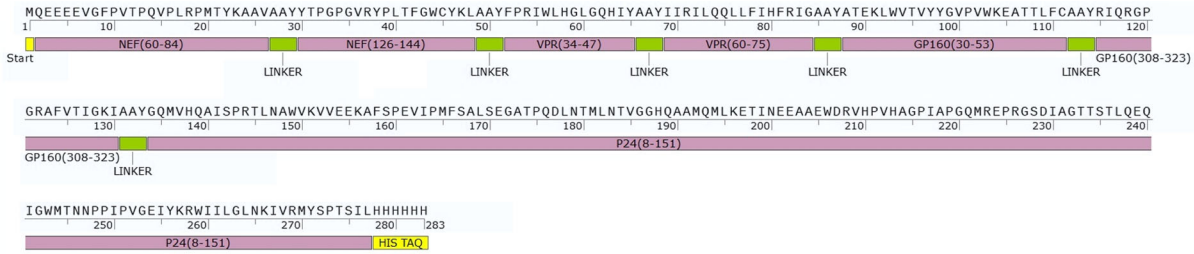

Fig. 2 The polyepitope peptide construct: the polyepitope peptide construct was designed using $Nef_{60–84}$, $Nef_{126–144}$, $Vpr_{34–47}$, $Vpr_{60–75}$, $Gp160_{30–53}$, $Gp160_{308–323}$ and $P24_{8–151}$ epitopes. The yellow color at the beginning of the peptide shows the first methionine amino acid. The yellow color at the end of the peptide shows 6xHis-tag. Green colors represent AAY linker between epitopes, which is the proteasome cleavage site, and the purple colors are related to the selected epitopes. The polyepitope peptide is 283 amino acids long with a molecular weight of ∼ 32 kDa

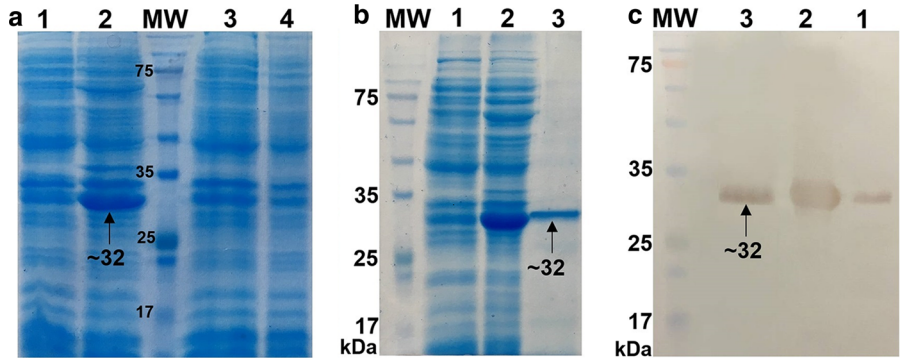

Fig. 4 Expression (**a**), purification (**b**), and western blotting (**c**) of the rNef-Vpr-Gp160-P24 peptide in Rosetta: **a** Lane 1: before induction in Rosetta containing pET-24a(+)-*nef-vpr-gp160-p24,* Lane 2: 4 h after induction in Rosetta containing pET-24a(+)-*nef-vpr-gp160-p24*, Lane 3: Before induction in Rosetta containing pET-24a(+), Lane 4: 4 h after induction in Rosetta containing pET-24a(+); **b** Lane 1: before induction, Lane 2: 4 h after induction, Lane 3: the purified rNef-Vpr-Gp160-P24 peptide; **c** Lane 1: before induction, Lane 2: 4 h after induction, Lane 3: the purified rNef-Vpr-Gp160-P24 peptide. MW: Molecular weight marker (prestained protein ladder, 10–180 kDa, Fermentas)

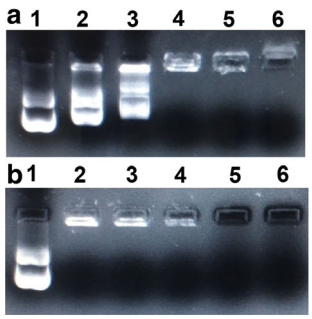

Fig. 5 Gel retardation assay of the MPG/DNA (**a**) and HR9/DNA (**b**) complexes: **a** Lane 1: pEGFP-N1-*nef-vpr-gp160-p24* (control), Lane 2: N/P: 0.5, Lane 3: N/P: 1, Lane 4: N/P: 2, Lane 5: N/P: 5, Lane 6: N/P: 10; **b** Lane 1: pEGFP-N1-*nef-vpr-gp160-p24* (control), Lane 2: N/P: 0.5, Lane 3: N/P: 1, Lane 4: N/P: 2, Lane 5: N/P: 5, Lane 6: N/P: 10

Zetasizer at the same ratios (Table 5). The pEGFP-N1-*nef-vpr-gp160-p24* (− 16.4 mV) and rNef-Vpr-Gp160-P24 (-26.8 mV) had negative charges, while the MPG/pEGFP-N1-*nef-vpr-gp160-p24* (22.8 mV), HR9/pEGFP-N1-*nef-vpr-gp160-p24* (22.8 mV), CyLo P-1/rNef-Vpr-Gp160-P24 (5.11 mV), and LDP-NPR/rNef-Vpr-Gp160-P24 (9.14 mV) complexes had positive charges that can be considered as an important factor for transferring the complexes through the cell membrane.

MTT assay

The results of cell viability showed that MPG, HR9, pEGFP-N1-*nef-vpr-gp160-p24*, MPG/pEGFP-N1-*nef-vpr-gp160-p24*, HR9/pEGFP-N1-*nef-vpr-gp160-p24*, CyLoP-1, LDP-NLS, rNef-Vpr-Gp160-P24, CyLoP-1/rNef-Vpr-Gp160-P24, and LDP-NLS/rNef-Vpr-Gp160-P24 had no major toxicity on the cells within 48 h ($p > 0.05$, Fig. 9).

Transfection of HEK-293 T cells with the MPG/DNA and HR9/DNA complexes

MPG and HR9 peptides were able to deliver pEGFP-N1-*nef-vpr-gp160-p24* to the cells, which ultimately led to the expression of the rNef-Vpr-Gp160-P24 polyepitope peptide in the cells. The transfected cells appeared as green areas in the fluorescent microscope images (Fig. 10). Flow cytometry results showed that the cellular uptake of TurboFect/pEGFP-N1, MPG/pEGFP-N1, HR9/pEGFP-N1, TurboFect/pEGFP-N1-*nef-vpr-gp160-p24*, MPG/pEGFP-N1-*nef-vpr-gp160-p24* and HR9/pEGFP-N1-*nef-vpr-gp160-p24* complexes were 75.7 ± 0.30%, 75 ± 1.03%, 46.33 ± 0.80%, 40.23 ± 0.92%, 20.65 ± 1.70%, and 23.20 ± 0.81%, respectively (Fig. 10). HR9 and MPG peptides did not show a significant difference in DNA delivery in vitro ($p > 0.05$). Expression of the rNef-Vpr-Gp160-P24 peptide in the cells was confirmed by western blot analysis. The rNef-Vpr-Gp160-P24 peptide was observed as a clear band of ∼ 59 kDa (peptide + GFP) in the cells treated with the complexes. No band was observed in untreated cells (Fig. 11a).

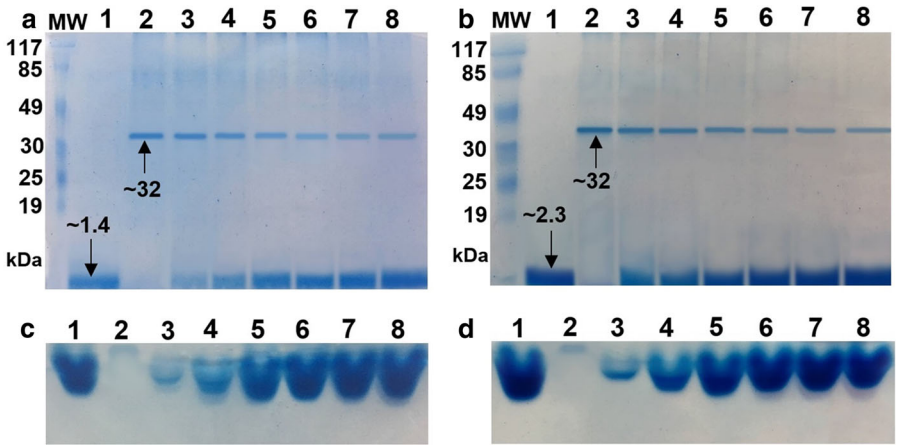

Fig. 6 Analysis of different molar ratios of the CyLoP-1/rNef-Vpr-Gp160-P24 (**a/c**) and LDP-NLS/rNef-Vpr-Gp160-P24 (**b/d**) complexes in SDS-PAGE (**a/b**) and native PAGE (**c/d**); (**a/c**): Lane 1: CyLoP-1 peptide (control), Lane 2: Purified rNef-Vpr-Gp160-P24 peptide (control), Lane 3: Molar ratio of 2, Lane 4: Molar ratio of 5, Lane 5: Molar ratio of 10, Lane 6: Molar ratio of 15, Lane 7: Molar ratio of 20, Lane 8: Molar ratio of 30; (**b/d**): Lane 1: LDP-NLS peptide (control), Lane 2: Purified rNef-Vpr-Gp160-P24 peptide (control), Lane 3: Molar ratio of 2, Lane 4: Molar ratio of 5, Lane 5: Molar ratio of 10, Lane 6: Molar ratio of 15, Lane 7: Molar ratio of 20, Lane 8: Molar ratio of 30. *MW* Molecular weight marker (Prestained protein ladder, 19–117 kDa, Maxcell)

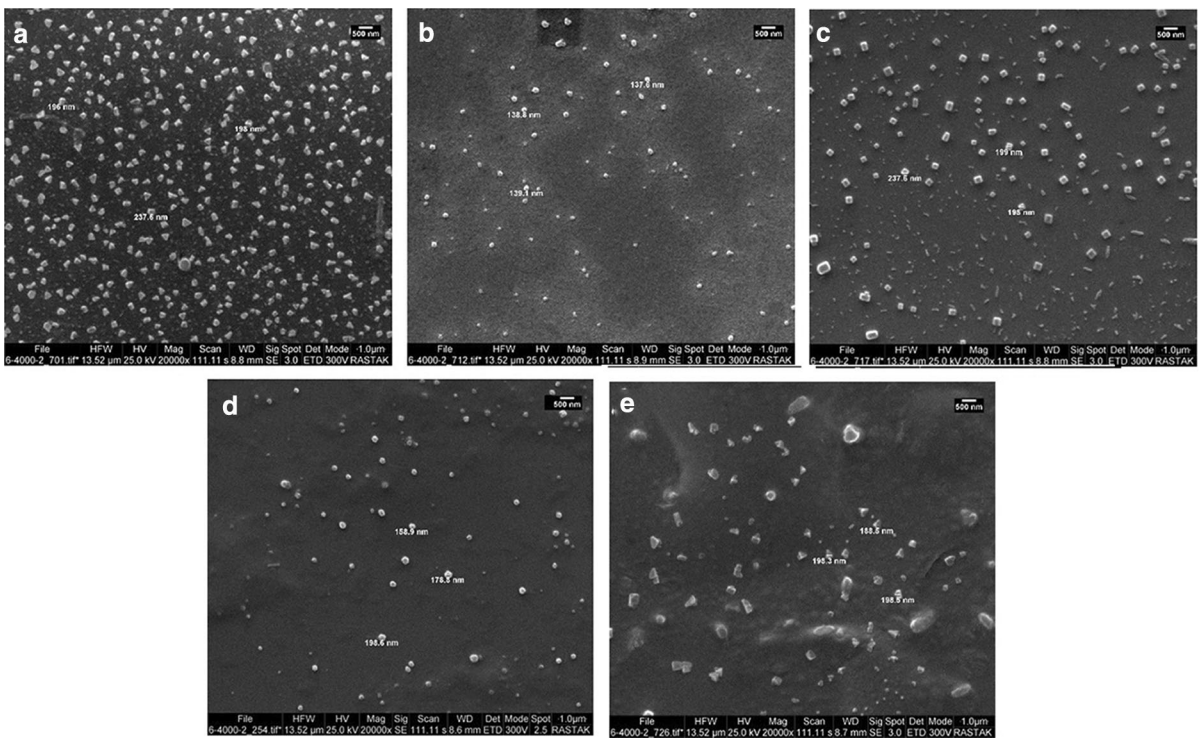

Fig. 7 The SEM micrograph of DNA and CPP nanoparticles: **a** pEGFP-N1-*nef-vpr-gp160-p24* (∼ 200–250 nm) **b** MPG (∼ 100–150 nm) **c** HR9 (∼ 150–250 nm) **d** MPG/pEGFP-N1-*nef-vpr-gp160-p24* (∼ 150–200 nm), and **e** HR9/pEGFP-N1-*nef-vpr-gp160-p24* (∼ 150–200 nm)

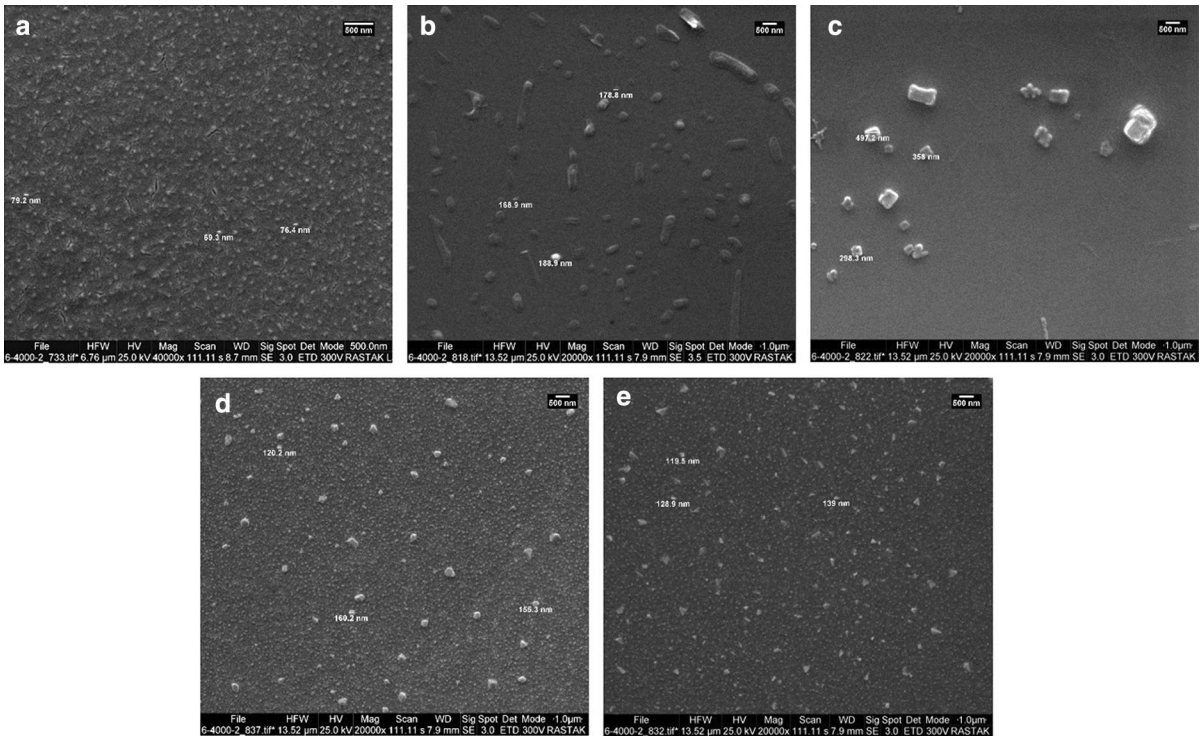

Fig. 8 The SEM micrograph of peptide and CPP nanoparticles: **a** rNef-Vpr-Gp160-P24 (∼ 50–100 nm) **b** CyLoP-1 (∼ 150–200 nm) **c** LDP-NLS (∼ 300–500 nm) **d** CyLoP-1/rNef-Vpr-Gp160-P24 (∼ 100–200 nm) **e** LDP-NLS/rNef-Vpr-Gp160-P24 (∼ 100–150 nm)

Table 5 Size and surface charge of nanoparticles measured by SEM and Zetasizer, respectively

Construct	Size (nm)	Surface charge (mV)
pEGFP-N1-*nef-vpr-gp160-p24*	200–250	− 16.4
pEGFP-N1-*nef-vpr-gp160-p24*/MPG	150–200	22.8
pEGFP-N1-*nef-vpr-gp160-p24*/HR9	150–200	22.8
rNef-Vpr-Gp160-P24	50–100	− 26.8
rNef-Vpr-Gp160-P24/CyLoP-1	100–200	5.11
rNef-Vpr-Gp160-P24/LDP-NLS	100–150	9.14

Transfection of HEK-293 T cells with the CyLoP-1/peptide and LDP-NLS/peptide complexes

The western blot results demonstrated that CyLoP-1 and LDP-NLS peptides were able to deliver rNef-Vpr-Gp160-P24 peptide to the cells 2 h after transfection. The rNef-Vpr-Gp160-P24 peptide was observed as a clear band of ∼ 32 kDa in the cells treated with the complexes. No band was observed in untreated cells (Fig. 11b).

Discussion

Over the past 30 years, many efforts have been performed to design an effective HIV vaccine, but no efficient vaccine has been developed. So far, several peptide vaccines have been designed including HIV-v (Vpr, Vif, Rev and Nef), C4-V3 (Gp120), VAC3S (Gp41), VACC-4X (p24Gag), F4/AS01B (p24, RT, Nef, and p17) and Afo-18, but the capacity of these vaccines was very limited to increase the HIV specific responses (Leal et al. 2017). Various bioinformatics methods have been developed to design

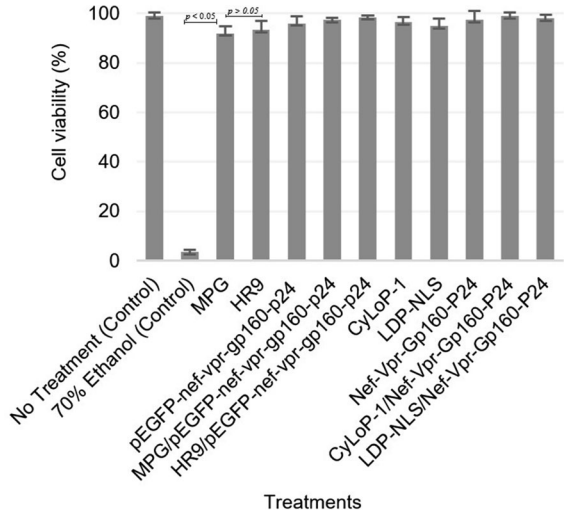

Fig. 9 MTT assay of the treated HEK-293 T cells: HEK-293 T cells were treated with MPG (41.5 µg), HR9 (9.3 µg), pEGFP-N1-*nef-vpr-gp160-p24* (2 µg), MPG/pEGFP-N1-*nef-vpr-gp160-p24* (N/P:10), HR9/pEGFP-N1-*nef-vpr-gp160-p24* (N/P:5), CyLoP-1 (10 µg), LDP-NLS (10 µg), rNef-Vpr-Gp160-P24 (1 µg), CyLoP-1/rNef-Vpr-Gp160-P24 (molar ratio of 10) and LDP-NLS/rNef-Vpr-Gp160-P24 (molar ratio of 10). The untreated HEK-293 T cells and the cells treated with 70% ethanol were considered as negative (100% cell viability) and positive controls, respectively

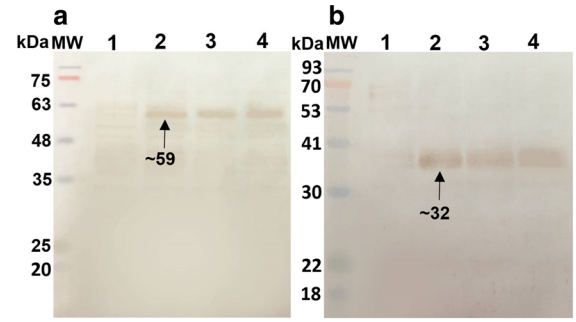

Fig. 11 Western blot analysis of HEK-293 T cells transfected with CPP/DNA (**a**) and CPP/peptide (**b**) complexes: **a** Lane 1: Untransfected cells (negative control), Lane 2: Cells transfected with MPG/pEGFP-N1-*nef-vpr-gp160-p24* complex, Lane 3: Cells transfected with HR9/pEGFP-N1-*nef-vpr-gp160-p24* complex, Lane 4: Cells transfected with TurboFect/pEGFP-N1-*nef-vpr-gp160-p24* complex (positive control); **b** Lane 1: Untransfected cells (negative control), Lane 2: Cells transfected with CyLoP-1/rNef-Vpr-Gp160-P24 complex, Lane 3: Cells transfected with LDP-NLS/rNef-Vpr-Gp160-P24 complex, Lane 4: Cells transfected with TurboFect/rNef-Vpr-Gp160-P24 complex (positive control). *MW* Molecular weight markers (prestained protein ladder, 10–245 kDa, Fermentas)

peptide vaccines. Advances in these methods have led to the development of more effective vaccines against hypervariable viruses such as HIV-1. One study demonstrated that the use of bioinformatics tools for the selection of conserved epitopes in combination with in vitro methods can accelerate the development of an HIV-1 vaccine (Degroot 2003). In this study, we used bioinformatics tools to design a polyepitope peptide vaccine based on HIV-1 conserved epitopes which had interaction with prevalent HLAs in Iran and the world. The $Nef_{134–144}$, $Vpr_{38–47,}$ and $Gp160_{37–46}$

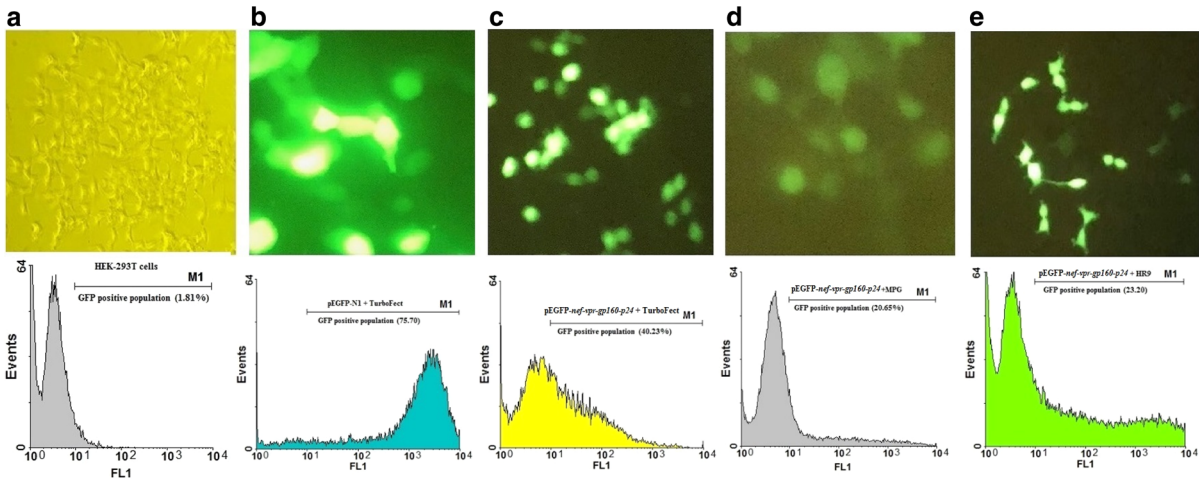

Fig. 10 Analysis of the transfected HEK-293 T cells using fluorescent microscopy and flow cytometry: **a** untransfected cells (negative control). **b** Cells transfected with TurboFect/pEGFP-N1 complex (positive control). **c** Cells transfected with TurboFect/pEGFP-N1-*nef-vpr-gp160-p24* complex (positive control). **d** Cells transfected with MPG/pEGFP-N1-*nef-vpr-gp160-p24* complex, and **e** Cells transfected with HR9/pEGFP-N1-*nef-vpr-gp160-p24* complex

epitopes had the highest MHCI binding level and the $Vpr_{65–82}$ epitope had the highest MHC II binding level. The $Vpr_{38–47}$ (98.89%) and $Vpr_{65–82}$ (97.55%) epitopes had the highest conservancy (Khairkhah et al. 2018). The selected immunodominant epitopes for the design of the polyepitope construct were $Nef_{60–84}$, $Nef_{126–144}$, $Vpr_{34–47}$, $Vpr_{60–75}$, $Gp160_{30–53}$, $Gp160_{308–323}$, and $P24_{8–151}$. The interaction between these epitopes and prevalent HLAs was studied using CABS-dock peptide-protein docking website. Using Docking, we detected the binding site of ligand on protein receptors and ranked the models based on CD and average RMSD. The $Vpr_{60–75}$ and $Vpr_{34–47}$ epitopes had the highest average CD in interaction with HLA I and HLA II, respectively. The highest quality of docking in interaction with HLA I and HLA II was related to $Nef_{60–84}$ and $Vpr_{60–75}$ with an average RMSD of 1.86 and 1.67, respectively.

On the other hand, we used cell-penetrating peptides to deliver the DNA and peptide constructs into HEK-293 T cells. MPG and HR9 peptides were used to transfer pEGFP-N1-*nef-vpr-gp160-p24* into the cells. MPG is an amphipathic peptide containing 27 amino acids and has three domains including a hydrophobic domain, a lysine-rich domain derived from the nuclear localization sequence (NLS) of SV40 and a linker (Saleh et al. 2015). These properties have made this peptide as an option for the delivery of oligonucleotides and plasmid DNA into different types of cells (Morris 1997). Cell-penetrating peptides could bind to biomolecules by covalent binding or forming non-covalent complexes (Kawamoto et al. 2011). Amphipathic peptides such as MPG formed stable non-covalent complexes with nucleic acids at certain N/P ratios (Layek et al. 2015). In one study, non-covalent interactions between MPG and plasmid DNA showed that there is a high affinity between CPP and charged molecules (Gros et al. 2006). In another study, it was determined that MPG is 80–95% efficient in the delivery of the luciferase gene (Simeoni 2003). The important benefits of non-covalent complexes are simple preparation and retention of cargo properties (Huang et al. 2015). Besides, R9 synthetic peptides (SR9) caused membrane instability, and created temporary pores for cell penetration (Herce et al. 2009). Histidine-rich R9 (HR9, CH5-R9-H5C) contains polyhistidine and nona arginine (R9) sequences that are surrounded by two cysteine residues (Liu et al. 2015). Adding poly-histidine sequences and cysteine residues to CPPs could increase the expression of DNA cargoes within the cell (Lo and Wang 2008). A study showed that HR9 facilitates cellular uptake of nanoscale materials (Huang et al. 2015). In this study, MPG and HR9 peptides were able to deliver pEGFP-N1-*nef-vpr-gp160-p24* into the HEK-293 T cells. Another study indicated that among four characterization methods (TEM, SEM, AFM and DLS), SEM was suitable for characterization of nanoparticles above 50 nm in diameter (Eaton et al. 2017). Our SEM results showed that the MPG/pEGFP-N1-*nef-vpr-gp160-p24* (N/P: 10) and HR9/pEGFP-N1-*nef-vpr-gp160-p24* complexes (N/P: 5) formed nanoparticles with a diameter of < 200 nm. The Zetasizer results indicated that the combination of negatively charged pEGFP-N1-*nef-vpr-gp160-p24* with positively charged MPG and HR9 peptides forms positively charged complexes that can pass through the plasma membrane. Several studies have suggested that nanoparticles with positive charges and a diameter of about 200 nm can pass efficiently through the membrane (Rejman et al. 2004; Conner and Schmid 2003; Karjoo et al. 2013). Moreover, SEM results indicated that the MPG/pEGFP-N1-*nef-vpr-gp160-p24* complexes were spherical and the HR9/pEGFP-N1-*nef-vpr-gp160-p24* complexes were nonspherical. In some studies, it has been reported that spherical nanoparticles were delivered better than non-spherical nanoparticles (Yoo, Doshi and Mitragotri 2011). In contrast, our fluorescence microscopy and flow cytometry results demonstrated that the transfection efficiency of MPG/pEGFP-N1-*nef-vpr-gp160-p24* ($\sim$ 20.65%) and HR9/pEGFP-N1-*nef-vpr-gp160-p24* ($\sim$ 23.20%) nanoparticles were approximately similar. Several studies have indicated that the transfection efficiency of CPPs depends on CPP and cargo properties, transfection conditions, and type of cells (Laufer and Restle 2008). Western blot analysis demonstrated that MPG and HR9 peptides could significantly deliver pEGFP-N1-*nef-vpr-gp160-p24* into the cells, and the rNef-Vpr-Gp160-P24-EGFP peptide was expressed in the cells similar to the cells transfected with the TurboFect/pEGFP-N1-*nef-vpr-gp160-p24* complex.

We used novel LDP-NLS and CyLoP-1 peptides to deliver rNef-Vpr-Gp160-P24 peptide into HEK-293 T cells. Cytosol localizing peptide-1 (CyLoP-1) is a cysteine-rich peptide derived from the NLS sequence of snake toxin called Crotamine (Ponnappan et al. 2017). Cysteine-rich peptides were used as agents for

delivery of biomolecules into cells (Mann et al. 2014). CyLoP-1 could pass through the plasma membrane at low concentrations (Jha et al. 2011). The efficient delivery of cargoes by CyLoP-1 was due to the presence of (RW) $_4$-K molecular motif (Bechara and Sagan 2013). The positive charge of particles could interact with the negative charge of the membrane and caused the endosomal lysis of the membrane (Rahmat et al. 2012). In one study, CyLoP-1 increased transfection and decreased cell cytotoxicity (Sabouri-Rad et al. 2017). In addition, LDP-NLS is a cell-penetrating peptide containing two parts of Latarcin-derived peptide (LDP) and the Nuclear Localization Sequence (NLS) of T40 antigen of the *simian virus* (Ponnappan and Chugh 2017). Latarsins are a group of spider venom toxins and have cell-penetrating and antimicrobial properties (Dubovskii et al. 2015). NLS alone has no cell penetrating property (Ragin, Morgan and Chmielewski 2002). The cell penetrating property of LDP was increased when bound to NLS. LDP-NLS could deliver protein cargoes into the cell (Ponnappan and Chugh 2017). In this study, CyLoP-1 and LDP-NLS peptides were able to transfer the rNef-Vpr-Gp160-P24 peptide into HEK-293 T cells. The CyLoP-1/rNef-Vpr-Gp160-P24 (molar ratio of 10) and LDP-NLS/rNef-Vpr-Gp160-P24 (molar ratio of 10) complexes formed stable nanoparticles with a diameter of < 200 nm. Zetasizer results demonstrated that the combination of the negatively charged rNef-Vpr-Gp160-P24 peptide with positively charged CyLoP-1 and LDP-NLS peptides formed positively charged complexes that can pass through the plasma membrane. Western blot results indicated that CyLoP-1 and LDP-NLS could deliver the rNef-Vpr-Gp160-P24 peptide into the cells similar to TurboFect.

In conclusion, we used bioinformatics tools to develop a polyepitope peptide construct containing the conserved immunogenic epitopes of HIV-1 subtypes. Docking results demonstrated that the polyepitope peptide (Nef-Vpr-Gp160-P24) interacts with prevalent HLAs in Iran and the world, so it can induce humoral and cellular immune responses in vivo. Besides, cell penetrating peptides (CPPs) were used to deliver the polyepitope DNA and peptide constructs into HEK-293 T cells. We used MPG and HR9 peptides for delivery of DNA (pEGFP-N1-*nef-vpr-gp160-p24*), and novel LDP-NLS and CyLoP-1 peptides for delivery of the polyepitope peptide (rNef-Vpr-Gp160-P24). These CPPs formed stable nanoparticles with pEGFP-N1-*nef-vpr-gp160-p24* and rNef-Vpr-Gp160-P24 peptide, and were able to deliver these constructs into HEK-293 T cells, and did not show any major cytotoxicity for the cells. Therefore, these CPPs could be used as options for delivery of DNA and peptide into cells. However, further studies are needed to evaluate the delivery of these constructs in vivo, and the stimulation of humoral and cellular immune responses against these nanoparticles.

Supporting information Supplementary Table 1—Top-ranked CABS-dock models of peptide-HLA I complexes.

Supplementary Table 2—Top-ranked CABS-dock models of peptide-HLA II complexes.

Compliance with ethical standards

Conflict of interest The authors declare no conflict of interest.

Ethical approval This article does not contain any studies with human participants or animals performed by any of the authors.

References

Arnon R, Ben-Yedidia T (2003) Old and new vaccine approaches. Int Immunopharmacol 3:1195–1204. https://doi.org/10.1016/s1567-5769(03)00016-x

Bechara C, Sagan S (2013) Cell-penetrating peptides: 20 years later, where do we stand? FEBS Lett 587:1693–1702. https://doi.org/10.1016/j.febslet.2013.04.031

Chin'Ombe N, Ruhanya V (2015) HIV/AIDS vaccines for Africa: scientific opportunities, challenges and strategies. Pan Afr Med J. https://doi.org/10.11604/pamj.2015.20.386.4660

Chiozzini C, Toschi E (2015) HIV-1 tat and immune dysregulation in AIDS pathogenesis: a therapeutic target. Curr Drug Targ 17:33–45. https://doi.org/10.2174/1389450116666150825110658

Conner SD, Schmid SL (2003) Regulated portals of entry into the cell. Nature 422:37–44. https://doi.org/10.1038/nature01451

Degroot A (2003) Mapping cross-clade HIV-1 vaccine epitopes using a bioinformatics approach. Vaccine 21:4486–4504. https://doi.org/10.1016/s0264-410x(03)00390-6

Dubovskii PV, Vassilevski AA, Kozlov SA et al (2015) Latarcins: versatile spider venom peptides. Cell Mol Life Sci 72:4501–4522. https://doi.org/10.1007/s00018-015-2016-x

Eaton P, Quaresma P, Soares C et al (2017) A direct comparison of experimental methods to measure dimensions of synthetic nanoparticles. Ultramicroscopy 182:179–190. https://doi.org/10.1016/j.ultramic.2017.07.001

Esparza J (2013) What has 30 years of HIV vaccine research taught us? Vaccines 1:513–526. https://doi.org/10.3390/vaccines1040513

Esteves A, Parreira R, Venenno T et al (2002) Molecular epidemiology of HIV type 1 infection in portugal: High prevalence of non-B subtypes. AIDS Res Hum Retroviruses 18:313–325. https://doi.org/10.1089/088922202753519089

Goede AD, Vulto A, Osterhaus A, Gruters R (2015) Understanding HIV infection for the design of a therapeutic vaccine. Part I: epidemiology and pathogenesis of HIV infection. Ann Pharm Françaises 73:87–99. https://doi.org/10.1016/j.pharma.2014.11.002

Gros E, Deshayes S, Morris MC, et al (2006) A non-covalent peptide-based strategy for protein and peptide nucleic acid transduction. Biochimica et Biophysica Acta (BBA)—Biomembranes 1758:384–393. https://doi.org/10.1016/j.bbamem.2006.02.006

Guidotti G, Brambilla L, Rossi D (2017) Cell-penetrating peptides: from basic research to clinics. Trends Pharmacol Sci 38:406–424. https://doi.org/10.1016/j.tips.2017.01.003

Hanna Z, Kay DG, Rebai N et al (1998) Nef harbors a major determinant of pathogenicity for an AIDS-like disease induced by HIV-1 in transgenic mice. Cell 95:163–175. https://doi.org/10.1016/s0092-8674(00)81748-1

Herce H, Garcia A, Litt J et al (2009) Arginine-rich peptides destabilize the plasma membrane, consistent with a pore formation translocation mechanism of cell-penetrating peptides. Biophys J 97:1917–1925. https://doi.org/10.1016/j.bpj.2009.05.066

Huang Y-W, Lee H-J, Tolliver LM, Aronstam RS (2015) Delivery of nucleic acids and nanomaterials by cell-penetrating peptides: opportunities and challenges. Biomed Res Int 2015:1–16. https://doi.org/10.1155/2015/834079

Jha D, Mishra R, Gottschalk S et al (2011) CyLoP-1: A novel cysteine-rich cell-penetrating peptide for cytosolic delivery of cargoes. Bioconjug Chem 22:319–328. https://doi.org/10.1021/bc100045s

Kaminchik J, Margalit R, Yaish S et al (1994) Cellular distribution of HIV type 1 Nef protein: Identification of domains in Nef required for association with membrane and detergent-insoluble cellular matrix. AIDS Res Hum Retroviruses 10:1003–1010. https://doi.org/10.1089/aid.1994.10.1003

Karjoo Z, Mccarthy HO, Patel P et al (2013) Systematic engineering of uniform, highly efficient, targeted and shielded viral-mimetic nanoparticles. Small 9:2774–2783. https://doi.org/10.1002/smll.201300077

Kawamoto S, Takasu M, Miyakawa T et al (2011) Inverted micelle formation of cell-penetrating peptide studied by coarse-grained simulation: importance of attractive force between cell-penetrating peptides and lipid head group. J Chem Phy 134:095103. https://doi.org/10.1063/1.3555531

Kelly J, Beddall MH, Yu D et al (2008) Human macrophages support persistent transcription from unintegrated HIV-1 DNA. Virology 372:300–312. https://doi.org/10.1016/j.virol.2007.11.007

Khairkhah N, Namvar A, Kardani K, Bolhassani A (2018) Prediction of cross-clade HIV-1 T cell epitopes using immunoinformatics analysis. Proteins 86:1284–1293. https://doi.org/10.1002/prot.25609

Kunwar P, Hawkins N, Dinges WL et al (2013) Superior Control of HIV-1 Replication by CD8 T cells targeting conserved epitopes: implications for HIV vaccine design. PLoS ONE. https://doi.org/10.1371/journal.pone.0064405

Kurcinski M, Jamroz M, Blaszczyk M et al (2015) CABS-dock web server for the flexible docking of peptides to proteins without prior knowledge of the binding site. Nucleic Acids Res. https://doi.org/10.1093/nar/gkv456

Laufer S, Restle T (2008) Peptide-mediated cellular delivery of oligonucleotide-based therapeutics *in vitro*: quantitative evaluation of overall efficacy employing easy to handle reporter systems. Curr Pharma Des 14:3637–3655. https://doi.org/10.2174/138161208786898806

Layek B, Lipp L, Singh J (2015) Cell penetrating peptide conjugated chitosan for enhanced delivery of nucleic acid. Int J Mol Sci 16:28912–28930. https://doi.org/10.3390/ijms161226142

Leal L, Lucero C, Gatell JM et al (2017) New challenges in therapeutic vaccines against HIV infection. Expert Rev Vaccines 16:587–600. https://doi.org/10.1080/14760584.2017.1322513

Li C, Shen Z, Li X et al (2012) Protection against SHIV-KB9 infection by combining rDNA and rFPV vaccines based on HIV multiepitope and p24 protein in chinese rhesus macaques. Clin Dev Immunol 2012:1–9. https://doi.org/10.1155/2012/958404

Liu BR, Chen HH, Chan MH et al (2015) Three arginine-rich cell-penetrating peptides facilitate cellular internalization of red-emitting quantum dots. J Nanosci Nanotechnol 15:2067–2078. https://doi.org/10.1166/jnn.2015.9148

Lo SL, Wang S (2008) An endosomolytic Tat peptide produced by incorporation of histidine and cysteine residues as a nonviral vector for DNA transfection. Biomaterials 29:2408–2414. https://doi.org/10.1016/j.biomaterials.2008.01.031

Lundberg P, Langel U (2003) A brief introduction to cell-penetrating peptides. J Mol Recognit 16:227–233. https://doi.org/10.1002/jmr.630

Mann A, Shukla V, Khanduri R et al (2014) Linear short histidine and cysteine modified arginine peptides constitute a potential class of DNA delivery agents. Mol Pharm 11:683–696. https://doi.org/10.1021/mp400353n

Miller RH, Sarver N (1997) HIV accessory proteins as therapeutic targets. Nat Med 3:389–394. https://doi.org/10.1038/nm0497-389

Milletti F (2012) Cell-penetrating peptides: classes, origin, and current landscape. Drug Discov Today 17:850–860. https://doi.org/10.1016/j.drudis.2012.03.002

Morris M (1997) A new peptide vector for efficient delivery of oligonucleotides into mammalian cells. Nucleic Acids Res 25:2730–2736. https://doi.org/10.1093/nar/25.14.2730

Motevalli F, Bolhassani A, Hesami S, Shahbazi S (2018) Supercharged green fluorescent protein delivers HPV16E7 DNA and protein into mammalian cells in vitro and in vivo. Immunol Lett 194:29–39. https://doi.org/10.1016/j.imlet.2017.12.005

Perrin H, Canderan G, Sékaly RP, Trautmann L (2010) New approaches to design HIV-1 T-cell vaccines. Curr Opin HIV AIDS 5:368–376. https://doi.org/10.1097/coh.0b013e32833d2cc0

Ponnappan N, Budagavi DP, Chugh A (2017) CyLoP-1: membrane-active peptide with cell-penetrating and antimicrobial properties. Biochimica et Biophysica Acta (BBA)—Biomembranes 1859:167–176. https://doi.org/10.1016/j.bbamem.2016.11.002

Ponnappan N, Chugh A (2017) Cell-penetrating and cargo-delivery ability of a spider toxin-derived peptide in mammalian cells. Eur J Pharm Biopharm 114:145–153. https://doi.org/10.1016/j.ejpb.2017.01.012

Pooga M, Langel Ü (2015) Classes of cell-penetrating peptides. Methods Mol Biol 1324:3–28. https://doi.org/10.1007/978-1-4939-2806-4_1

Puls RL, Emery S (2006) Therapeutic vaccination against HIV: current progress and future possibilities. Clin Sci 110: 59–71. https://doi.org/10.1042/cs20050157

Ragin AD, Morgan RA, Chmielewski J (2002) Cellular import mediated by nuclear localization signal peptide sequences. Chem Biol 9:943–948. https://doi.org/10.1016/s1074-5521(02)00189-8

Rahmat D, Khan MI, Shahnaz G et al (2012) Synergistic effects of conjugating cell penetrating peptides and thiomers on non-viral transfection efficiency. Biomaterials 33:2321–2326. https://doi.org/10.1016/j.biomaterials.2011.11.046

Rejman J, Oberle V, Zuhorn IS, Hoekstra D (2004) Size-dependent internalization of particles via the pathways of clathrin- and caveolae-mediated endocytosis. Biochem J 377:159–169. https://doi.org/10.1042/bj20031253

Requejo HIZ (2006) Worldwide molecular epidemiology of HIV. Rev de Saúde Pública 40:331–345. https://doi.org/10.1590/s0034-89102006000200023

Sabouri-Rad S, Oskuee RK, Mahmoodi A et al (2017) The effect of cell penetrating peptides on transfection activity and cytotoxicity of polyallylamine. BioImpacts 7:139–145. https://doi.org/10.15171/bi.2017.17

Saleh T, Bolhassani A, Shojaosadati SA, Aghasadeghi MR (2015) MPG-based nanoparticle: an efficient delivery system for enhancing the potency of DNA vaccine expressing HPV16E7. Vaccine 33:3164–3170. https://doi.org/10.1016/j.vaccine.2015.05.015

Simeoni F (2003) Insight into the mechanism of the peptide-based gene delivery system MPG: implications for delivery of siRNA into mammalian cells. Nucleic Acids Res 31:2717–2724. https://doi.org/10.1093/nar/gkg385

Temsamani J, Vidal P (2004) The use of cell-penetrating peptides for drug delivery. Drug Discov Today 9:1012–1019. https://doi.org/10.1016/s1359-6446(04)03279-9

Wei B, Arora V, Foster J et al (2003) *In vivo* analysis of Nef function. Curr HIV Res 1:41–50. https://doi.org/10.2174/1570162033352057

Yoo JW, Doshi N, Mitragotri S (2011) Adaptive micro and nanoparticles: temporal control over carrier properties to facilitate drug delivery. Adv Drug Deliv Rev 63:1247–1256. https://doi.org/10.1016/j.addr.2011.05.004

Zorko M, Langel U (2005) Cell-penetrating peptides: mechanism and kinetics of cargo delivery. Adv Drug Deliv Rev 57:529–545. https://doi.org/10.1016/j.addr.2004.10.010